

On the reduced sensitivity of the Atlantic overturning to Greenland ice sheet melting in projections: a multi-model assessment

Didier Swingedouw · Christian B. Rodehacke ·
Steffen M. Olsen · Matthew Menary · Yongqi Gao ·
Uwe Mikolajewicz · Juliette Mignot

Received: 14 February 2014 / Accepted: 21 July 2014 / Published online: 26 August 2014
© Springer-Verlag Berlin Heidelberg 2014

Abstract Large uncertainties exist concerning the impact of Greenland ice sheet melting on the Atlantic meridional overturning circulation (AMOC) in the future, partly due to different sensitivity of the AMOC to freshwater input in the North Atlantic among climate models. Here we analyse five projections from different coupled ocean–atmosphere models with an additional 0.1 Sv (1 Sv = 10^6 m³/s) of freshwater released around Greenland between 2050 and 2089. We find on average a

further weakening of the AMOC at 26°N of 1.1 ± 0.6 Sv representing a 27 ± 14 % supplementary weakening in 2080–2089, as compared to the weakening relative to 2006–2015 due to the effect of the external forcing only. This weakening is lower than what has been found with the same ensemble of models in an identical experimental set-up but under recent historical climate conditions. This lower sensitivity in a warmer world is explained by two main factors. First, a tendency of decoupling is detected between the surface and the deep ocean caused by an increased thermal stratification in the North Atlantic under the effect of global warming. This induces a shoaling of ocean deep ventilation through convection hence ventilating only intermediate levels. The second important effect concerns the so-called Canary Current freshwater leakage; a process by which additionally released freshwater in the North Atlantic leaks along the Canary Current and escapes the convection zones towards the subtropical area. This leakage is increasing in a warming climate, which is a consequence of decreasing gyres asymmetry due to changes in Ekman pumping. We suggest that these modifications are related with the northward shift of the jet stream in a warmer world. For these two reasons the AMOC is less susceptible to freshwater perturbations (near the deep water formation sides) in the North Atlantic as compared to the recent historical climate conditions. Finally, we propose a bilinear model that accounts for the two former processes to give a conceptual explanation about the decreasing AMOC sensitivity due to freshwater input. Within the limit of this bilinear model, we find that 62 ± 8 % of the reduction in sensitivity is related with the changes in gyre asymmetry and freshwater leakage and 38 ± 8 % is due to the reduction in deep ocean ventilation associated with the increased stratification in the North Atlantic.

Electronic supplementary material The online version of this article (doi:[10.1007/s00382-014-2270-x](https://doi.org/10.1007/s00382-014-2270-x)) contains supplementary material, which is available to authorized users.

D. Swingedouw (✉)
EPOC laboratory, CNRS / University of Bordeaux, Allée
Geoffroy Saint Hilaire, Bordeaux 33615, France
e-mail: didier.swingedouw@u-bordeaux1.fr

C. B. Rodehacke · S. M. Olsen
DMI, Copenhagen, Denmark

C. B. Rodehacke · U. Mikolajewicz
Max-Planck-Institut für Meteorologie, Hamburg, Germany

M. Menary
Hadley Centre, Exeter, UK

Y. Gao
NERSC, Bergen, Norway

J. Mignot
LOCEAN Laboratory, Sorbonne Universités (UPMC,
Univ Paris 06)-CNRS-IRD-MNHN,
4 Place Jussieu, Paris, France

J. Mignot
Climate and Environmental Physics, Physics Institute
and Oeschger Centre of Climate Change Research,
University of Bern, Bern, Switzerland

Keywords Greenland ice sheet melting · Thermohaline circulation · Oceanic gyre · Ocean–atmosphere interactions · Oceanic dynamics · Sea-level rise · AMOC · North Atlantic

1 Introduction

Projections from the Coupled Model Intercomparison Project (CMIP) have shown that the Atlantic Meridional Overturning Circulation (AMOC) might weaken substantially in the coming century. CMIP3 projected a weakening of around 30 % of the AMOC in 2100 (Schneider et al. 2007) with a considerable spread among models. Within the CMIP5 database, this estimation remains conclusive with a reduced spread among models and a better agreement with AMOC estimates (Weaver et al. 2012). Nevertheless, these projections usually neglect any melt water from continuing intensified melting of the Greenland ice sheet (GrIS).

Recent observations, on the other hand, show such a melting, and even suggest an accelerating melt rate during the last decades (Rignot et al. 2011). Bamber et al. (2012) reveal that most of this melting is released into the Irminger Sea where it might induce a pronounced change in ocean hydrography by 2025 that could be larger than any observed past Great Salinity Anomalies (e.g. Belkin et al. 1998). For the year 2100, Schrama and Wouters (2011) project a global sea-level rise of 35 cm due to GrIS melting as compared to present day, which equals a melting rate rising to 0.08 Sv (1 Sv = 10⁶ m³/s) in 2100.

Using a very large ensemble of models from the CMIP3 or earlier generations, Stouffer et al. (2006) showed that such a freshwater input in the North Atlantic could induce a significant weakening of the AMOC. Nevertheless they have also shown that the impact under preindustrial conditions largely depends on the model considered. Indeed, after 100 years of 0.1 Sv freshwater hosing, they found a weakening of the AMOC intensity ranging from approximately 1–10 Sv. A large spread across models was also identified in a set of impact simulations to GrIS mass loss under present-day climate conditions in Swingedouw et al. (2013, S2013 hereafter). This latter study analysed the response of six different models to identical melt water forcing. The coordinated set-up across both state-of-the-art climate models and ocean-only models imposed 0.1 Sv of freshwater distributed equally around Greenland for four decades.

No consensus has been reached about the impact of GrIS melting on the future AMOC. Using a single model with different magnitude of freshwater input, Fichefet et al. (2003), Swingedouw et al. (2006), Hu et al. (2011) and Driesschaert et al. (2007) found a noticeable impact of GrIS melting in the coming centuries, while Winguth

et al. (2005), Ridley et al. (2005), Jungclaus et al. (2006), Mikolajewicz et al. (2007) and Vizcaíno et al. (2010) found almost no significant additional AMOC weakening in various projections. Thus, it seems necessary to consider different models under identical GrIS melting conditions in order to better evaluate the uncertainties concerning the future of the AMOC due to different model sensitivities to freshwater input in the North Atlantic.

The sensitivity of models to freshwater release in the North Atlantic depends on the considered climate state. For instance, Swingedouw et al. (2009) using the IPSLCM4 model found that AMOC sensitivity to fresh water is larger for LGM climate than for warmer climate like present day or last interglacial, confirming findings from Ganopolski and Rahmstorf (2001) using a simplified model. Van Meerbeeck et al. (2011) using LOVECLIM model found that during glacial time the AMOC was more sensitive during milder climate for Marine Isotope Stage 3 (MIS3, between around 28–60 kyr BP) than during the last glacial maximum. This result offers an explanation why Dansgaard–Oeschger instabilities were more clearly expressed during MIS3.

In this study, we address specifically the following question: what is the effect of melt water input from Greenland on the AMOC under strong warming conditions in a multi-model ensemble? In terms of experimental design, this work is the direct continuation of the impact study performed under present-day climate conditions in S2013.

2 Experimental design

We consider projections performed using five different coupled climate models participating in CMIP5 and/or CMIP3, namely EC-Earth, MPI-ESM, HadCM3, IPSL-CM5A-LR and BCM2. For a description of the different models used, the reader is referred to S2013. All the simulations start from spin-up simulations followed by historical simulations from 1850 up to 2006. Afterwards, they have been forced by the RCP8.5 scenario (RCP stands for representative concentration pathway, the number 8.5 represents an estimate of the top of the atmosphere radiative forcing at the year 2100 in W/m², cf. Moss et al. 2010) over the period 2006–2100. BCM2 is an exception, because the historical forcings are imposed until 2000 only and afterwards the A1B scenario (based on a balanced emphasis on all energy sources, cf. Morita et al. 2011) is imposed until 2100. From these projections (here called FutCon), impact experiments (FutHos) have been launched in 2050, when additional runoff is released homogeneously along Greenland's coast with a constant rate of 0.1 Sv for 40 years. In 2090 this corresponds to a global sea-level rise of 35 cm as compared to present day, consistent with projections of Schrama and Wouters (2011).

Table 1 Description of the main simulations discussed in this paper and in S2013 (Swingedouw et al. 2013)

	S2013		This paper	
	Control	Hosing	Control	Hosing
Description	Historical forcings 1850–2005	Historical forcings plus 0.1 Sv hosing 1965–2004	RCP8.5 (A1B for BCM2) forcings 2006–2100	RCP8.5 forcings plus 0.1 Sv hosing 2050–2089
Designation	HisCon	HisHos	FutCon	FutHos

These different twenty-first century sensitivity experiments are also evaluated against the twentieth century reference simulations discussed in S2013. The compilation of experiments is summarized in Table 1.

The tailored GrIS mass loss model projections represent a high-end impact scenario in terms of the excess melt considered. This experimental set up constitutes, to our knowledge, the first multi-model ensemble aimed at evaluating the impact of a large GrIS melting on the AMOC at the end of the twenty-first century. In addition, the identical freshwater release design here and in S2013 allows evaluating the AMOC sensitivity to freshwater input under different transient climates. Ultimately it sheds light on the question about the susceptibility of the ocean and the interconnected climate system to fresh water disturbances under the current and future warming climates. This study is complementary to what has been done in Stouffer et al. (2006) for the pre-industrial conditions.

3 Results

3.1 Response to increase in greenhouse gases

We first compare the response among the models to the increase in external forcing alone (FutCon experiments). Simulated global climate averaged over the years 2091–2100 has warmed in the different models by 1.9–4.1 °C as compared to 2006–2015 (Fig. 1a, solid lines) with a mean of 3.4 ± 0.9 °C (3.5 – 4.1 °C with a mean of 3.8 ± 0.3 °C if only the four RCP8.5 simulations are considered). During this time period, the AMOC maximum at 26°N has weakened in all the models by 4.1 ± 1.7 Sv (Fig. 1b, solid lines) or a 29 ± 8 % decrease, in line with results from Schneider et al. (2007) for CMIP3 models and Weaver et al. (2012) for CMIP5 models.

This weakening of the AMOC is related with an increased North Atlantic stratification (Fig. 2). Comparing convection in FutCon against HisCon shows reduced areas of ventilation by convection (Fig. 3). Thus, the volume of water ventilated in winter by convection decreases (Fig. 4) and so the formation rate of North Atlantic deep water (NADW) feeding the lower limb of the AMOC. The density evolution of spatially averaged water column in the North Atlantic (70°E–20°W;

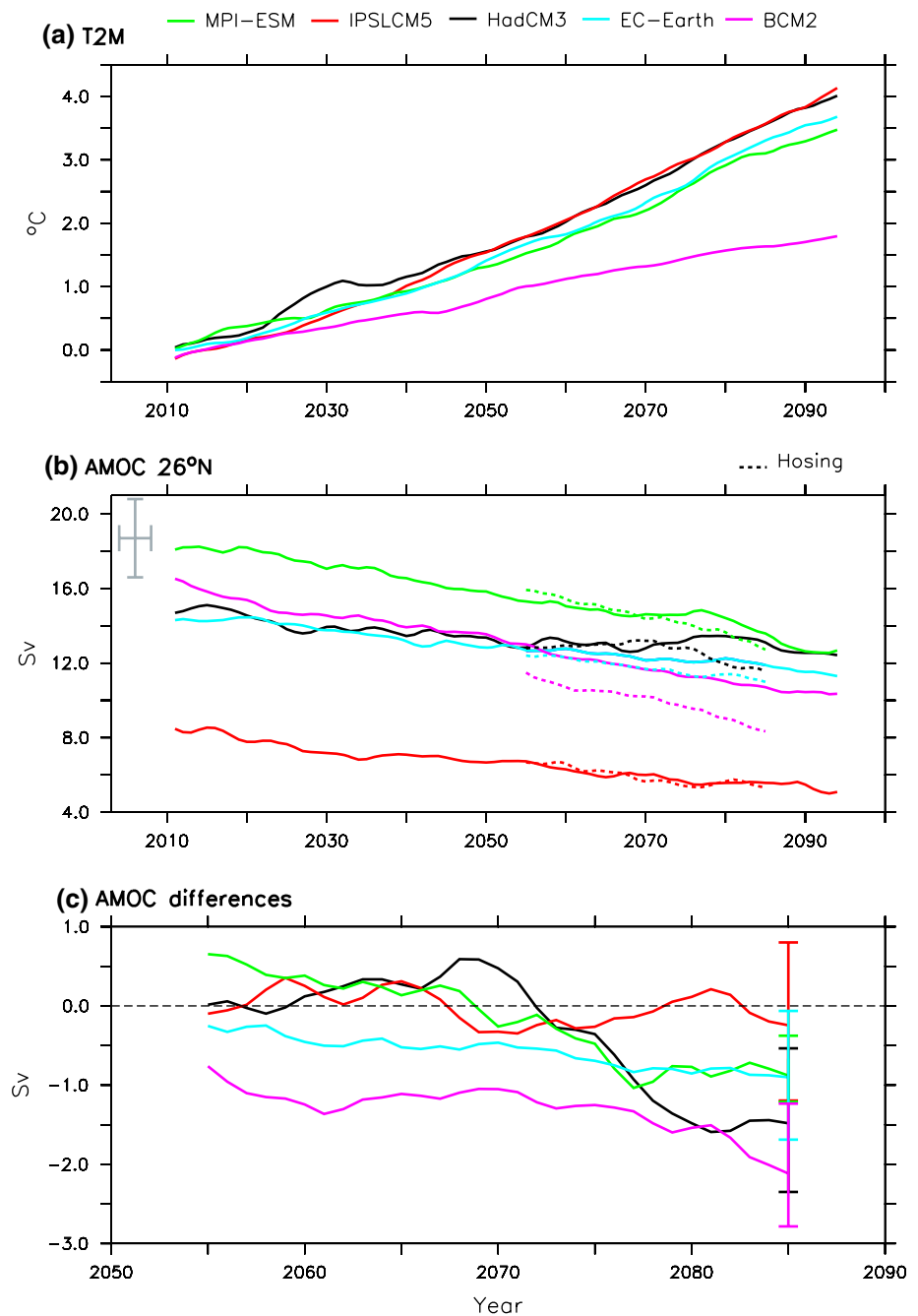
45°N–80°N) above and below 1,000 m supports this interpretation. In the upper 1,000 m, the density decreases by 0.21 ± 0.05 kg/m³ in FutCon while the density of water masses below are marginally lighter (0.03 ± 0.01 kg/m³, Fig. 2). In order to disentangle the role of salinity and temperature to the increased stratification, we linearize the density and computed separately the haline and thermal contributions. This approach (Fig. 5) highlights clearly that the increased stratification is predominantly driven by the changing temperature and, in particular, the warming of the surface ocean. In contrast, the simulated salinity does not even show a consistent response across models. The thermal changes increase the stratification by 0.17 ± 0.09 kg/m³ while the haline changes the density only by 0.01 ± 0.05 kg/m³ on average. Note that the haline contribution is largest in BCM2, where the warming is markedly lower than the rest of the models, which is partly explained by the use of a different forcing protocol. Considering positive feedbacks, whereby enhanced thermal stratification, for instance, may result in reduced vertical mixing favouring increased haline stratification in net precipitative regions, a weakening of the overturning circulation may also enhance the haline stratification (Mikolajewicz and Voss 2000). The present result therefore emphasizes the fact that the warming regulates the AMOC response in projections.

This chain of processes and its interpretation is consistent with the study of Gregory et al. (2005), for instance, who identified a dominant role of heat flux changes in explaining the AMOC weakening in CMIP3 projections. The differences between the models concerning the haline contribution to density changes are regulated by the opposing effects of the enhanced evaporation in the tropics, which tends to make the surface water masses flowing towards the deep water formation sites saltier in the Northern Atlantic on the one hand (Fig. 6) and a strengthened freshwater continental runoff supplied by enhanced precipitation in the high latitudes on the other hand. These effects compete in the North Atlantic when the hydrological cycle intensifies in a warming world (Durack et al. 2012).

3.2 Effect of GrIS melting in a warming world

After up to 40 years of on-going 0.1 Sv freshwater hosing around Greenland's coasts, the AMOC reduces

Fig. 1 Temporal evolution of **a** global mean 2-m air temperature and **b** AMOC maximum at 26°N in the different models for the FutCon (*solid*) and FutHos (*dashed*) simulations. **c** Differences in AMOC maximum at 26°N between melt water impact and control simulations (FutHos – FutCon) over the period 2050–2089. A 10-year running mean filter has been applied to all the time series. The AMOC estimate at 26°N from Kanzow et al. (2010) for the period 2004–2008 is represented as *grey cross* in (b). *Error bars* in (c) represent two standard deviations of the AMOC computed from the HisCon simulations (Swingedouw et al. 2013: S2013)



additionally by 1.1 ± 0.6 Sv over the period 2080–2089 at 26°N (Fig. 1c, 1.3 ± 1 Sv for the maximum AMOC value in the North Atlantic). This represents a further weakening of 27 ± 14 % in FutHos as compared to the reduction in FutCon between 2089–2100 and 2006–2015. If we restrict the focus only on the period when the additional runoff is applied (time frame 2080–2089 minus 2050–2059), the AMOC reduction at 26°N by the freshwater even reaches 122 ± 67 % of greenhouse warming effect (0.9 ± 0.6 Sv), which means that the additional AMOC weakening due to

the hosing in the ensemble mean is even slightly larger than the AMOC weakening in response to increasing radiative forcing.

This additional weakening is consistent with previous water hosing experiments (see introduction) and is attributed to the spreading of the freshwater to affect the upper water column in large parts of the North Atlantic (Fig. 7). The freshwater anomaly flows initially with the Greenland boundary current systems and only gradually entrains central parts of the subpolar gyre and the cyclonic gyres of the

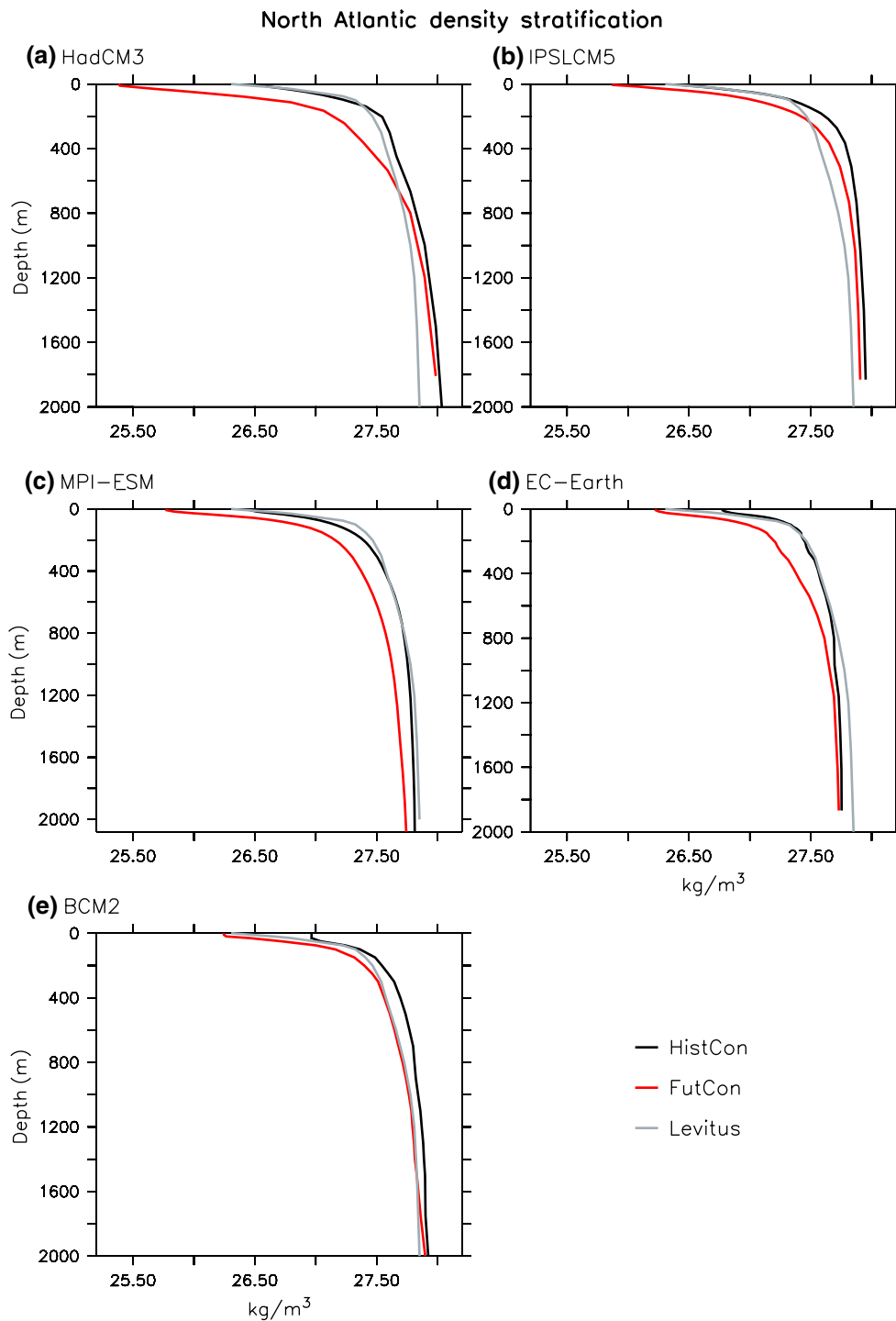


Fig. 2 Density profiles in the historical (HisCon) and projection simulations (FutCon) in standard configuration (i.e. without additional FW hosing) averaged over 40 years of simulations (1965–2004 for historical and 2050–2089 for projection simulations) and for the Lev-

itus (1998) climatology for the North Atlantic region (70°E–20°W; 45°N–80°N). **a** HadCM3, **b** IPSLCM5, **c** MPI-ESM, **d** EC-Earth and **e** BCM2

Nordic Seas. Thereby the additional freshwater eventually impacts the convective activity in winter in the North Atlantic (Fig. 3) as the ventilated water masses. Note that part of the freshwater anomaly does not remain in the subpolar

area but rather leaks toward the subtropical gyre along the Canary Current (Fig. 7) and hence represents an important sink for the freshwater out of the subpolar gyre (S2013). This point will be further discussed below.

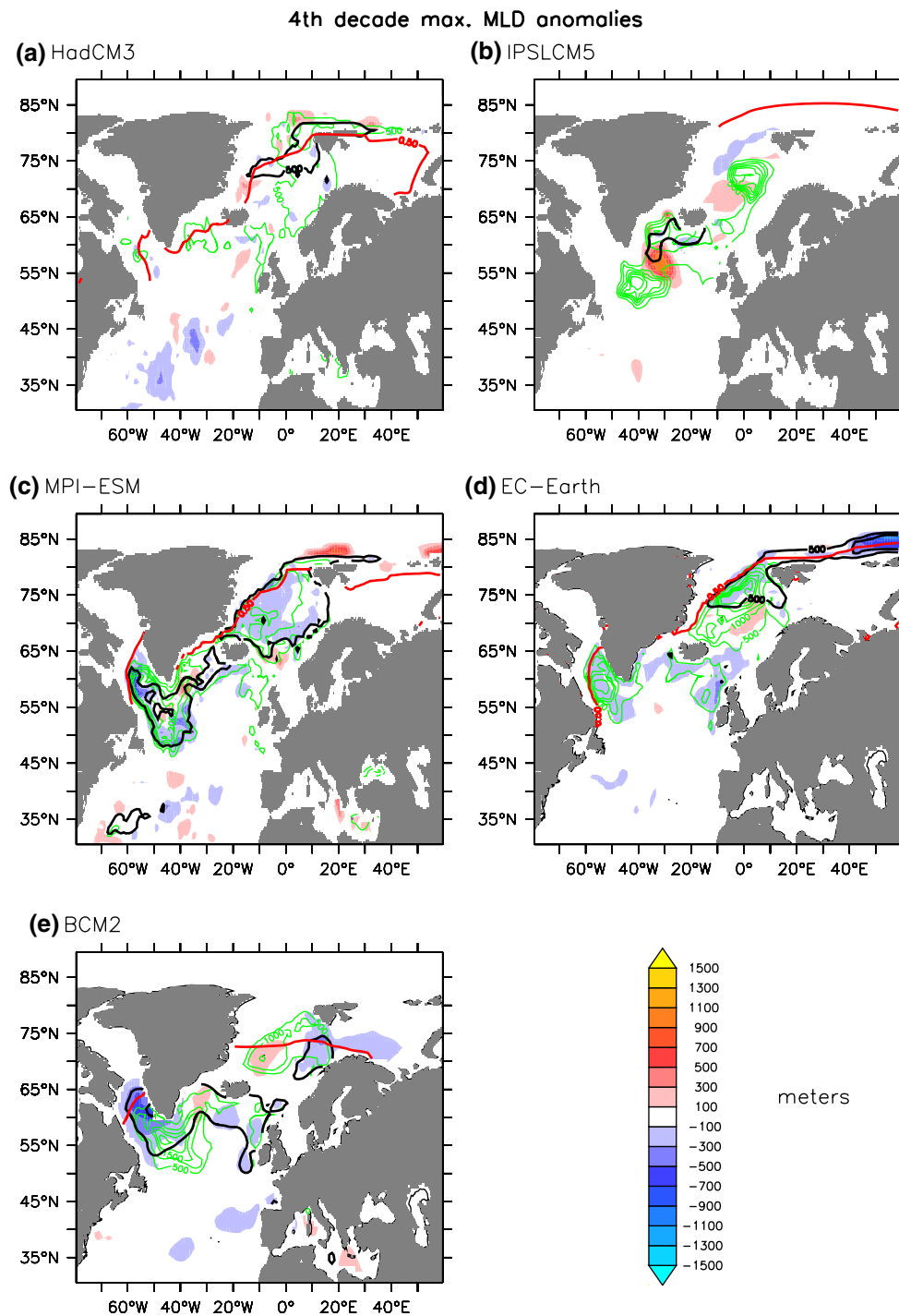


Fig. 3 Differences in the annual maximum of the mixed layer depth between FutHos and FutCon experiments averaged over the 4th decade (2080–2089) for the different models (unit: meter). *Black contoured lines* are annual maximum of the mixed layer depth over the period 2050–2089 in the FutCon experiments and the *green contour*

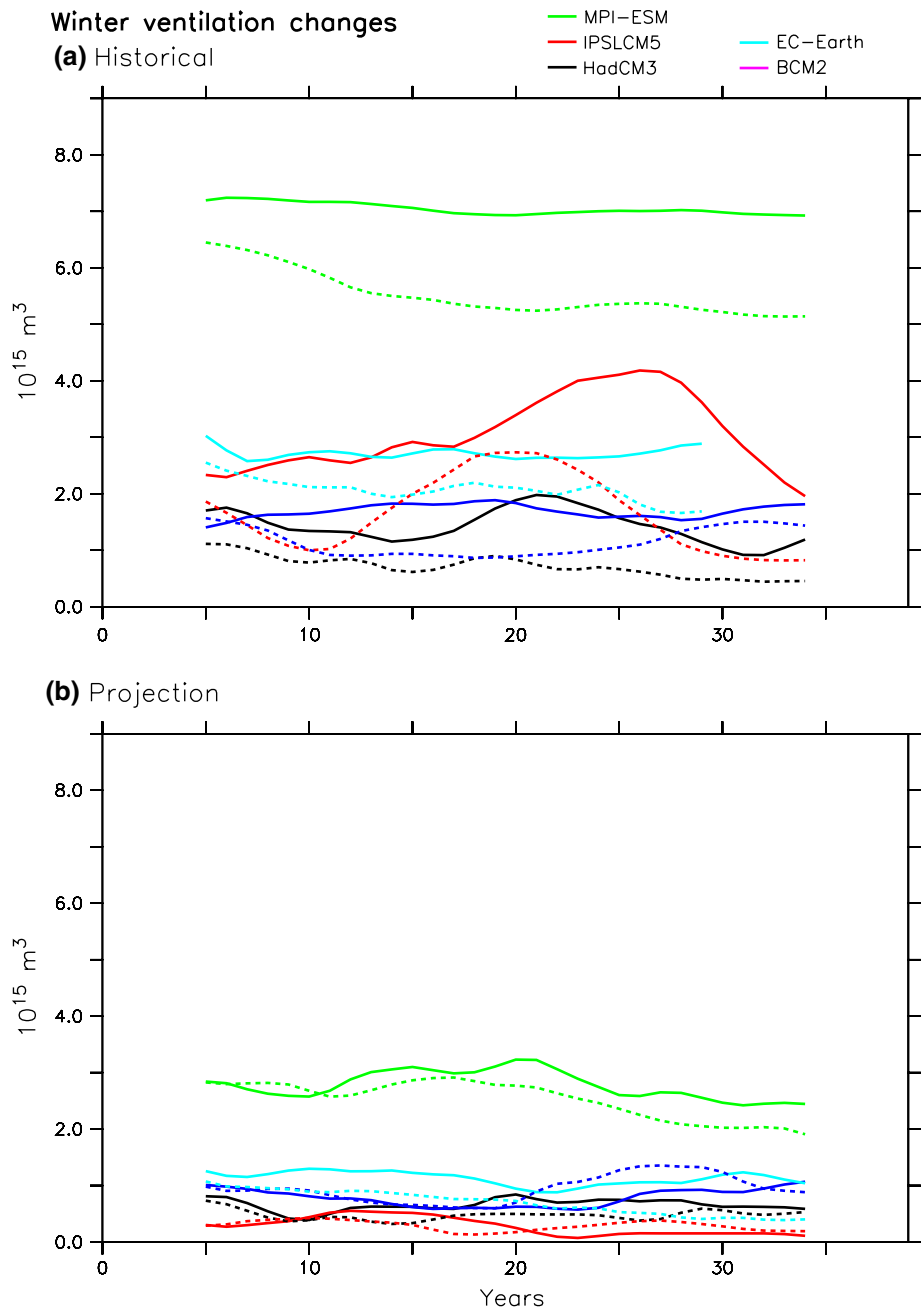
lines in the HisCon simulations over the period 1965–2004. The colour interval is 200 m and the contour line interval is 500 m. The *red line* represents the annual mean sea-ice edge (defined as the 50 % coverage) averaged over the years 2050–2089 of the FutCon experiments

3.3 Comparison with present-day sensitivity

The average AMOC weakening at 26°N after 40 years of hosing in the FutHos experiments is smaller by $58 \pm 23 \%$

than the reported averaged AMOC weakening at 26°N of 2.6 ± 1.7 Sv in the historical experiments of S2013 (HisHos-HisCon, cf. Table 1; Fig. 8). This result is not affected by the AMOC index chosen since the reduction

Fig. 4 Volume of water ventilated in the North Atlantic (in 10^{15} m^3) defined as the volume of water included in the mixed layer in winter when this layer is deeper than 300 m (running mean of 10 years). **a** Historical simulations with HisCon in *solid lines* and HisHos in *dashed lines*. And **b** projections with FutCon in *solid lines* and FutHos in *dashed lines*



concerns predominately the whole northern limb of the AMOC (not shown). The spread among the models is also reduced in the future experiments (FutHos-FutCon) as compared to historical experiments (HisHos-HisCon); with a standard deviation among the models almost three times lower (Fig. 8).

On decadal timescales, changes in density in the North Atlantic are related to AMOC changes (e.g. Swingedouw et al. 2007). Indeed, the water hosing induced AMOC changes are highly correlated ($r = 0.92$) in our multi-model ensemble with density changes in the North Atlantic averaged over the entire water column (Fig. 9). To uncover the

contribution of different processes we decompose these density changes over the North Atlantic into its haline and thermal components. This decomposition (Fig. 10) clearly reveals the importance of the salinity changes on the AMOC sensitivity to freshwater input in the North Atlantic across all models and under all analysed climate scenarios.

Indeed, when comparing hosing and control experiments in both climatic conditions, most of the density changes are related with the salinity component changes, the thermal component being of second order (Fig. 10). At first sight, we can explain this fact by the impact of freshwater released around Greenland on the North Atlantic salinity.

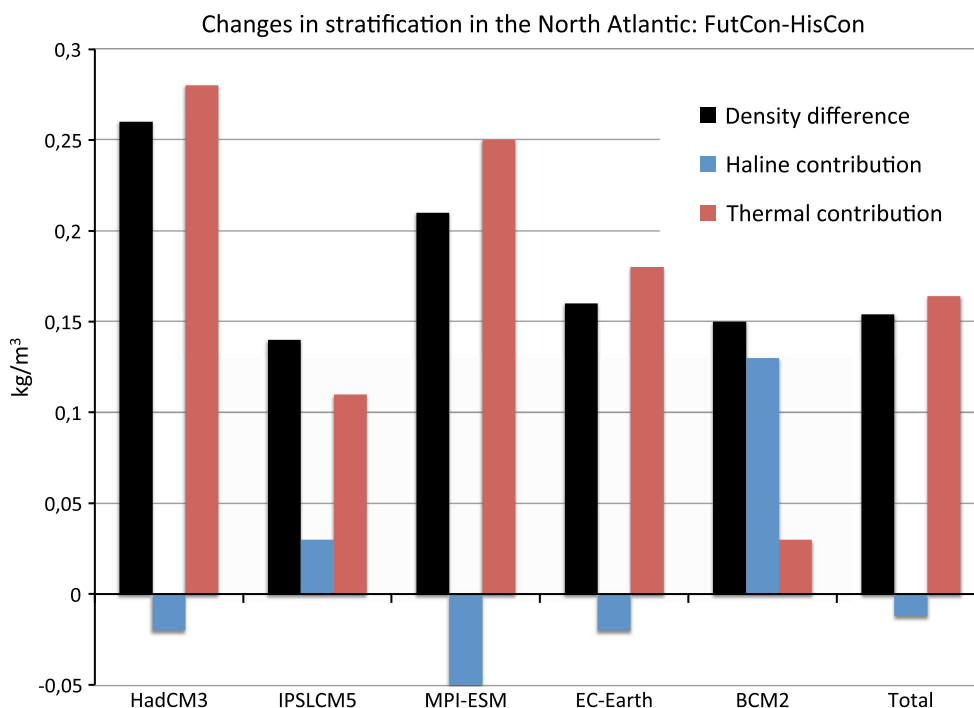


Fig. 5 Density differences between historical and RCP8.5 for the top 1,000 m minus density below 1,000 m averaged over the North Atlantic region (70°E–20°W; 45°N–80°N) as represent in Fig. 2 for the different models and the ensemble mean (column total). A linearization

of density with respect to salinity and temperature has been done. The *blue* and *red bars* correspond to the haline and thermal components respectively, while the black line is the total density changes. All these contributions are expressed in kg/m³

Nevertheless, we also notice that the decrease of AMOC sensitivity to freshwater input in a warmer world (comparison of FutHos-FutCon and HisHos-HisCon) is mainly due to salinity changes as well, although the freshwater input is the same between the two climatic conditions. Indeed the salinity component decrease is of 17.6 g/m³ in HisHos-HisCon and halved to only 8.3 g/m³ in FutHos-FutCon, while the changes in thermal component remains smaller. The total surface freshwater changes in the North Atlantic in the hosing simulations cannot explain such a difference since the totally released fresh water amount is identical under the two climatic conditions (not shown). Therefore, we argue that the salinity changes between the two climate configurations is due to salinity redistribution processes, either barotropic or baroclinic advection. On the southern border, the barotropic salinity transport can be related with the gyre circulation, while the baroclinic transport is associated with the overturning itself, which can be considered as an internal feedback of the AMOC system (Swingedouw et al. 2007). Unfortunately, not enough data from all the models are available to compute a proper budget of the salinity changes in the North Atlantic and of the former two components (although we do apply this kind of analysis for IPSL-CM5 model, see below).

Nevertheless, we hypothesize two main processes that may cause the weaker sensitivity of the AMOC to enhanced

fresh water discharge by elevated GrIS melting under a warmer climate. The first one is linked to the thermal effect of global warming on the oceanic stratification in the sub-polar area, which reduces ventilation of the deep ocean affecting the AMOC internal feedback of salinity transport. The second is the consequence of a modified mean state in the North Atlantic in a warmer world, which may favour the subtropical leakage of the imposed freshwater forcing and can be related with the gyre salinity transport from the former decomposition.

3.4 Reduction of deep ventilation in a warmer world

The differences of the oceanographic conditions between FutCon and HisCon may explain the changes in mixed layer depth and deep ventilation in the North Atlantic. Indeed, the links between the surface and the deep ocean are considerably weaker in FutCon compared to HisCon, because newly formed dense water masses reach henceforth intermediate levels in FutCon (Fig. 3) and overflow water masses, which are formed in the Nordic Seas, passing the Greenland-Iceland-Scotland Ridge ventilate less of the deep North Atlantic. The volume of ventilated water in winter (defined as the volume of water where the mixed layer depth exceeds 300 m) averaged over the North Atlantic declines by three-quarters from $3.44 \pm 1.86 \times 10^{15} \text{ m}^3$

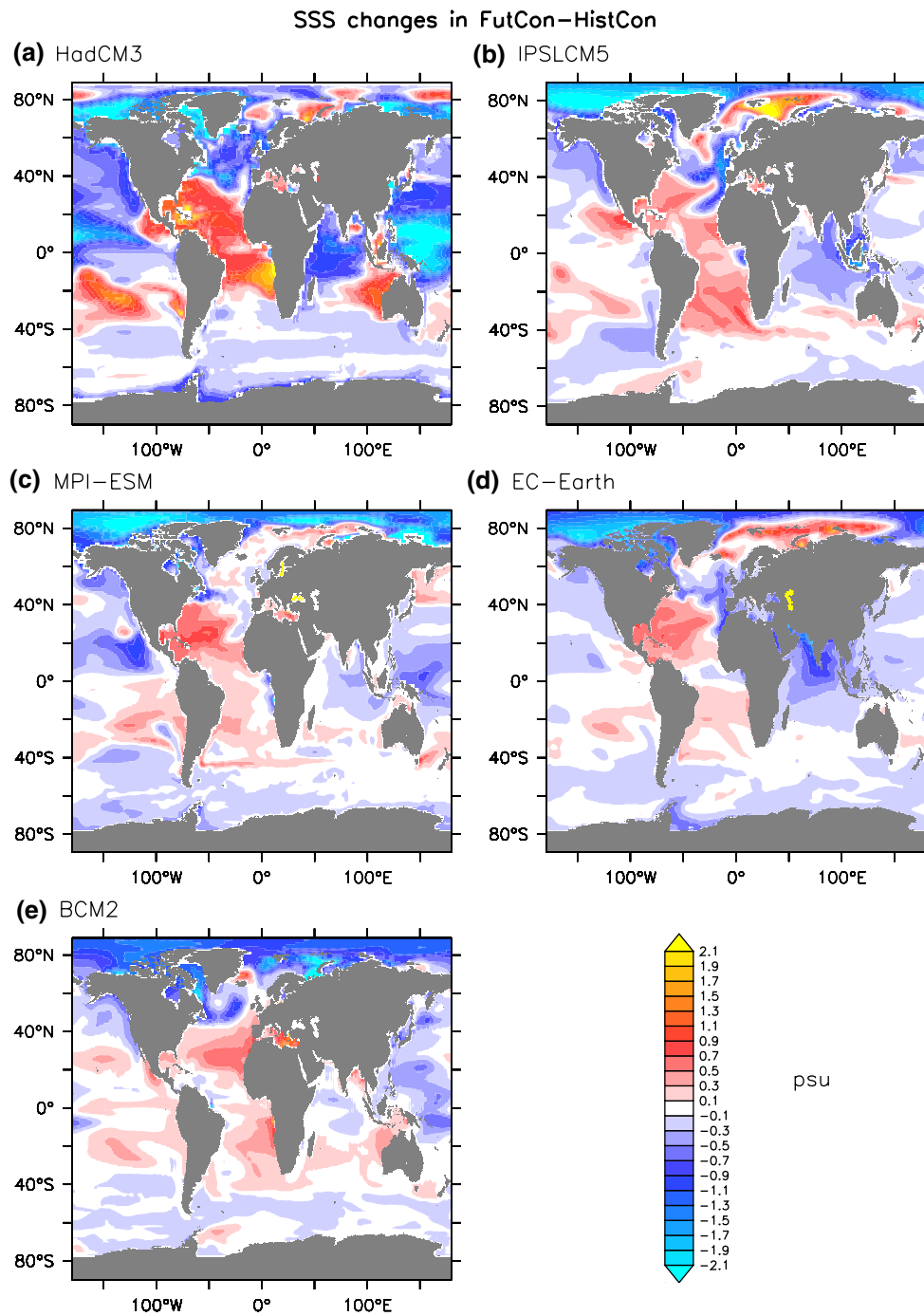


Fig. 6 Sea surface salinity (SSS) changes in the different projections without GrIS melting averaged over the years 2050–2089 as compared to SSS in historical simulations averaged over years 1965–2004

(cf. S2012). **a** HadCM3, **b** IPSLCM5, **c** MPI-ESM, **d** EC-Earth and **e** BCM2. The colour interval is 0.2 psu. These changes reflect the influence of the enhanced hydrological cycle

in the HisCon experiments (averaged over years 1965–2004) to $0.87 \pm 0.85 \times 10^{15} \text{ m}^3$ in the FutCon experiments (averaged over years 2050–2089). In all the models this decline is driven by a shallower convection, in particular in the Labrador Sea (Fig. 3). Ultimately this is reflected by the stronger stratified ocean under a warmer climate

(Fig. 2), which is predominately driven by rising surface layer temperatures as discussed above. Such an increase of stratification probably enhances the time residence of surface waters where the atmosphere freshens them, which may further decrease their salinity and strengthen the stratification. Nevertheless, the increase in stratification

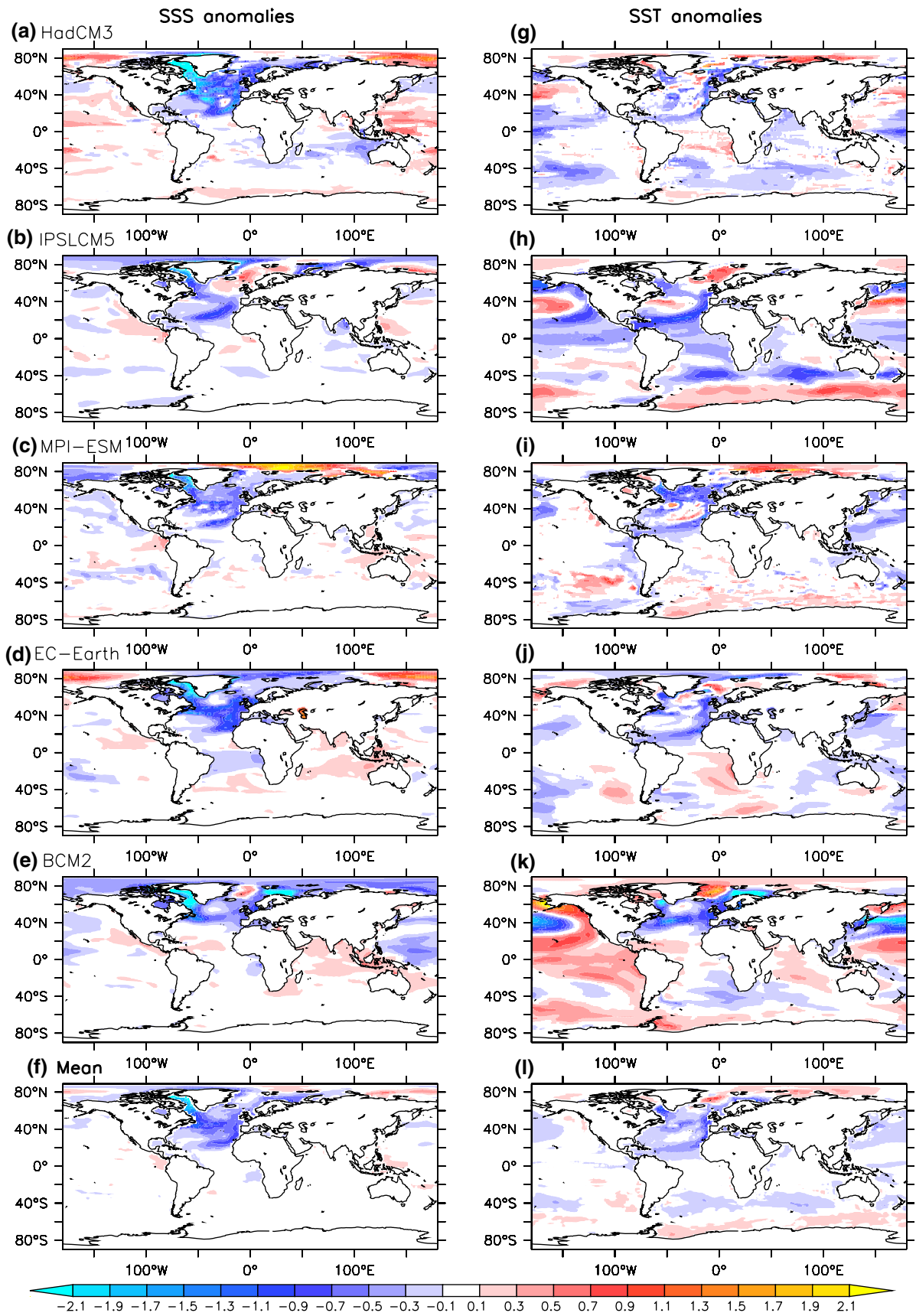


Fig. 7 Sea surface salinity (SSS) (*left*) and sea surface temperature (SST) (*right*) difference between FutHos and FutCon experiments averaged over the 4th decade (2080–2089) for the different models (a–e and g–k). Only the 95 % significant anomalies following a student *t* test are shown. The colour interval is 0.2 PSU for SSS and 0.2 °C for SST. The ensemble mean is shown in (f) for SSS and in (l) for SST

diminishes the amount of ventilated waters that can be affected by the freshening and therefore the impact of the latter on convection. This second process can be viewed as a kind of saturation of the hosing effect due to large decrease in convection under the dominant effect of

global warming, and therefore convection sites can be less affected. This process can be viewed as opposing the first effect of global warming on haline stratification, described e.g. in Mikolajewicz and Voss (2000). In other words since the ties between the deep and surface ocean are weakened, this effect results in a lower sensitivity of the AMOC to freshwater perturbations. This is particularly pronounced in IPSLCM5, which exhibits the largest decrease in ventilation under future global warming conditions. However a bolstered fresh water cap formed by the additional fresh water further decreases the linkage between the surface and deep ocean, because under the FutHos simulations

Fig. 8 Time evolution of the ensemble mean of differences in the AMOC maximum at 26°N between hosing and control simulations for the 5 coupled models considered here. The overlap represents the two-sigma uncertainty or spread among the models. In red is the ensemble mean for the FutHos-FutCon and in black is HisHos-HisCon

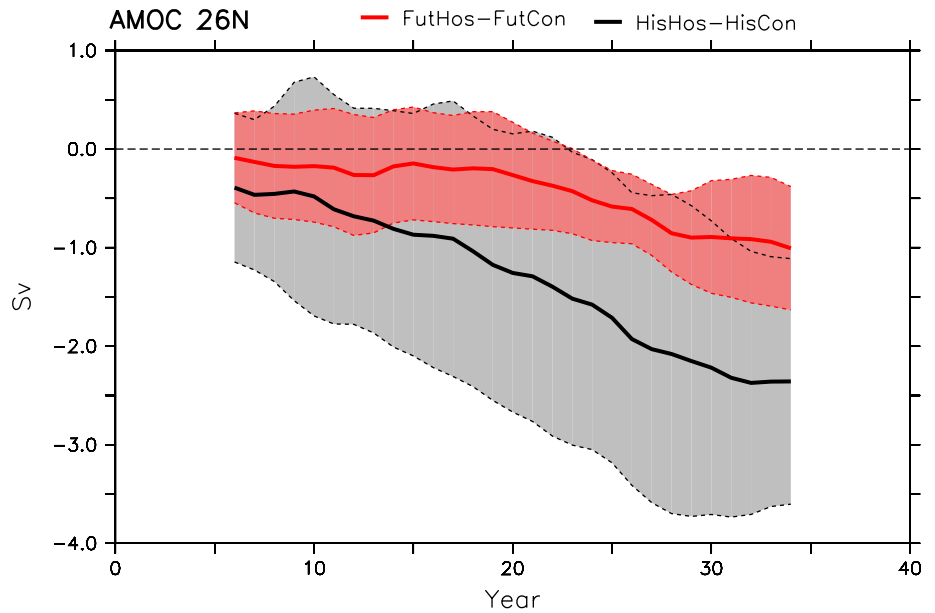
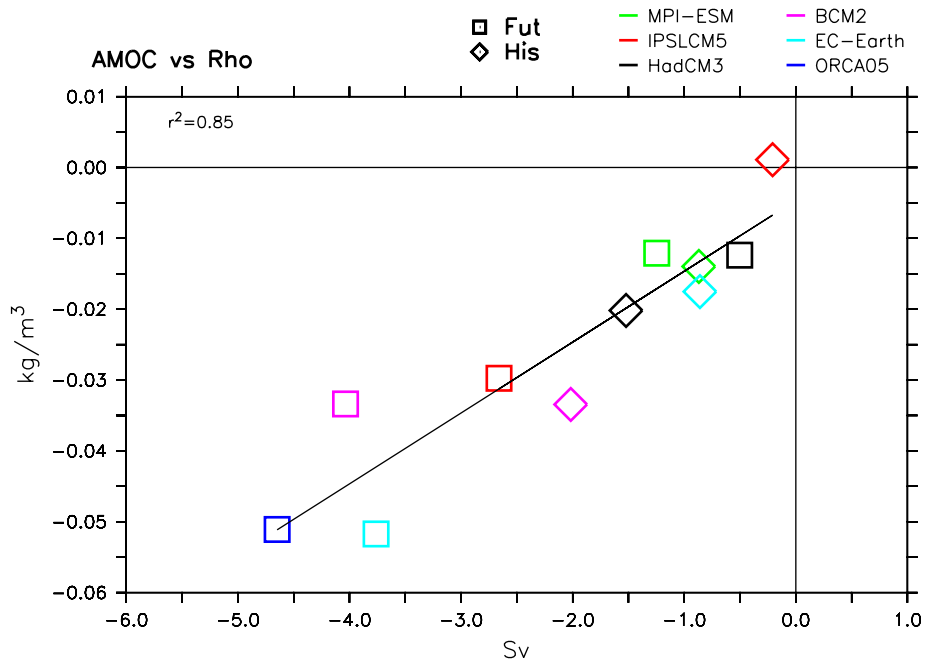


Fig. 9 AMOC changes versus density changes in the North Atlantic (70°E–20°W; 45°N–80°N) averaged from the top to the bottom; 4th decade mean. The AMOC changes are defined as the difference between the melt water impact and control projections for the AMOC maximum at 26°N. The black lines are a least squares linear regression made with the 11 couples of simulations ($r^2 = 0.85, p < 0.01$)



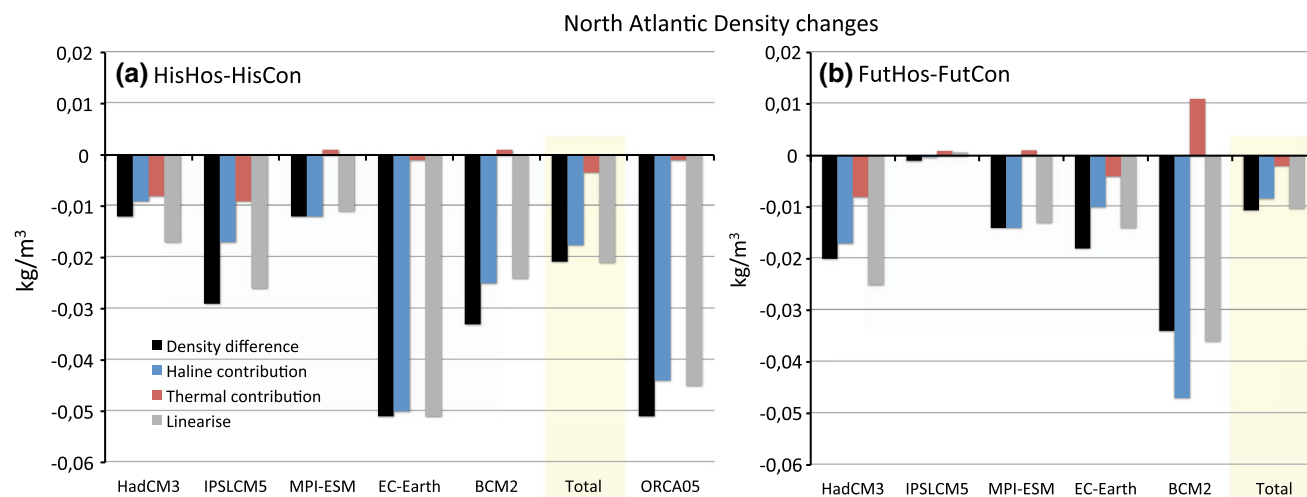


Fig. 10 North Atlantic density changes averaged over the whole column for the last decade **a** HisHos-HisCon and **b** (FutHos-FutCon). A linearization of density with respect to salinity and temperature has been done. The *blue* and *red* bars correspond to the haline and thermal components respectively, while the *black* line is the total density

changes while the *grey* line is the linearized density changes (sum of haline and thermal component). All these contributions are expressed in kg/m^3 . The columns total stands for the ensemble mean of all the coupled simulations (excluding ORCA05 for **a**)

the ventilated volume drops by an additional $25 \pm 6 \%$ ($0.17 \pm 0.04 \times 10^{15} \text{ m}^3$) over the last decade (2080–2089). This distinct reduction under the projections is less than the reduction of $39 \pm 13 \%$ ($1.35 \pm 0.46 \times 10^{15} \text{ m}^3$) during the historical period (HisHos versus HisCon). Nevertheless, we note that the changes in the AMOC are not simply linearly related with deep-water ventilation changes (Fig. 11), indicating that it is possible that other processes play a role.

In the projections, we also note that the shallower persisting convection is aligned along the receding sea-ice edge. This is particularly striking in the EC-Earth model, where convection moves northward out of the Barents Sea with the retreating sea-ice edge (Fig. 3). The Barents Sea is less affected by the freshening around Greenland compared to S2013, which may also explain less entrainment into the dense water sphere and mediate the moderate impact of GrIS melting.

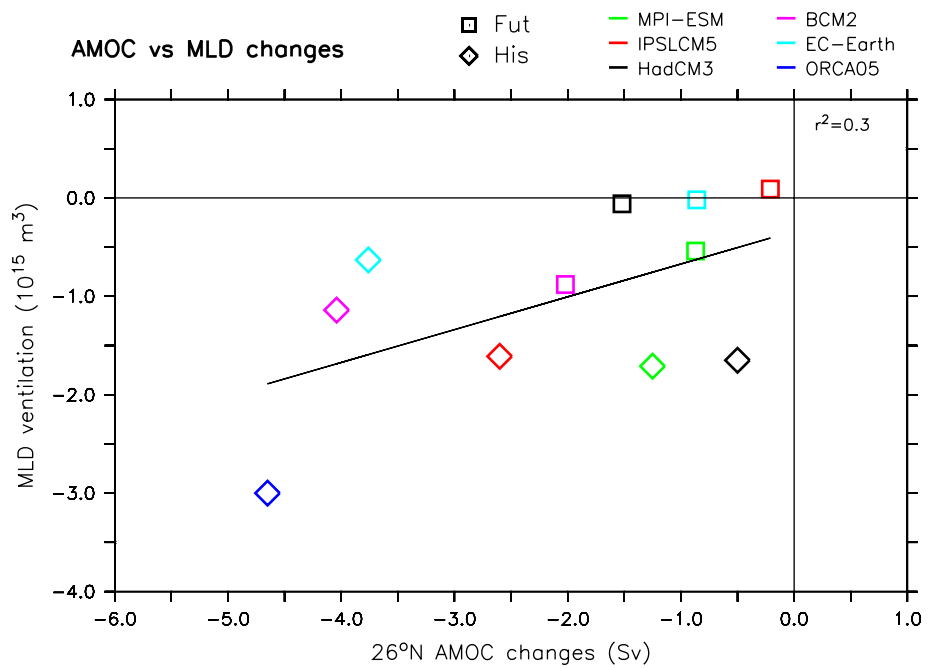
When looking at Fig. 9, it is clear that the models showing the largest changes in AMOC sensitivity to freshwater input are BCM2, EC-Earth and IPSL-CM5. These three models also have the main characteristic of losing most of their convective activity in or close to the Labrador Sea. Indeed, Fig. 3 shows that convection was very active in HisCon in the Labrador Sea and almost vanished in FutCon in the three models. Indeed, this convection site is known to be quite sensitive to climate change (*cf.* Wood et al. 1999), which may explain why the decrease is larger in this sea than in the Nordic Seas. The Labrador Sea is also very sensitive to freshwater input around Greenland as shown in S2013, so that the loss of convective activity in

the projections may explain the decrease of sensitivity to freshwater input in the three most sensitive models and thus in our ensemble.

3.5 Reduction of gyre asymmetry in a warmer world

Under historical climate conditions, S2013 have shown that the fresh water leakage from the subpolar gyre along the Canary Current is decisive for the AMOC quantitative response in our impact simulations. This new set of simulations is still in agreement with this finding as shown in Fig. 12. An animation available in supplementary materials shows the evolution of ensemble mean salinity anomalies with time and clearly the advective process by which salinity anomalies goes from the subpolar gyre towards the subtropical along the Canary Current, with a subduction towards deeper levels all along this path. Furthermore, as illustrated in the ensemble mean response (Fig. 7, bottom row), this freshwater leakage is associated with a negative sea surface temperature (SST) anomaly (Fig. 71). S2013 had found that the intensity of this leakage could be linked to the latitudinal orientation of the subpolar and subtropical boundary, which is related with the gyre asymmetry. Here again, strong leakage (negative values in Fig. 12a) is obtained by weak asymmetry (near-zonal gyre–gyre boundary), yielding a weaker AMOC sensitivity to imposed freshwater. In the projections however, we find an increase in this leakage (Fig. 12a) and a decrease in the gyre asymmetry (Fig. 12b) compared to present-day simulations (HisCon). This is especially pronounced in BCM2. As hypothesized in S2013, these interlinked

Fig. 11 Same as Fig. 9 but between deep-water ventilation and AMOC changes at 26°N



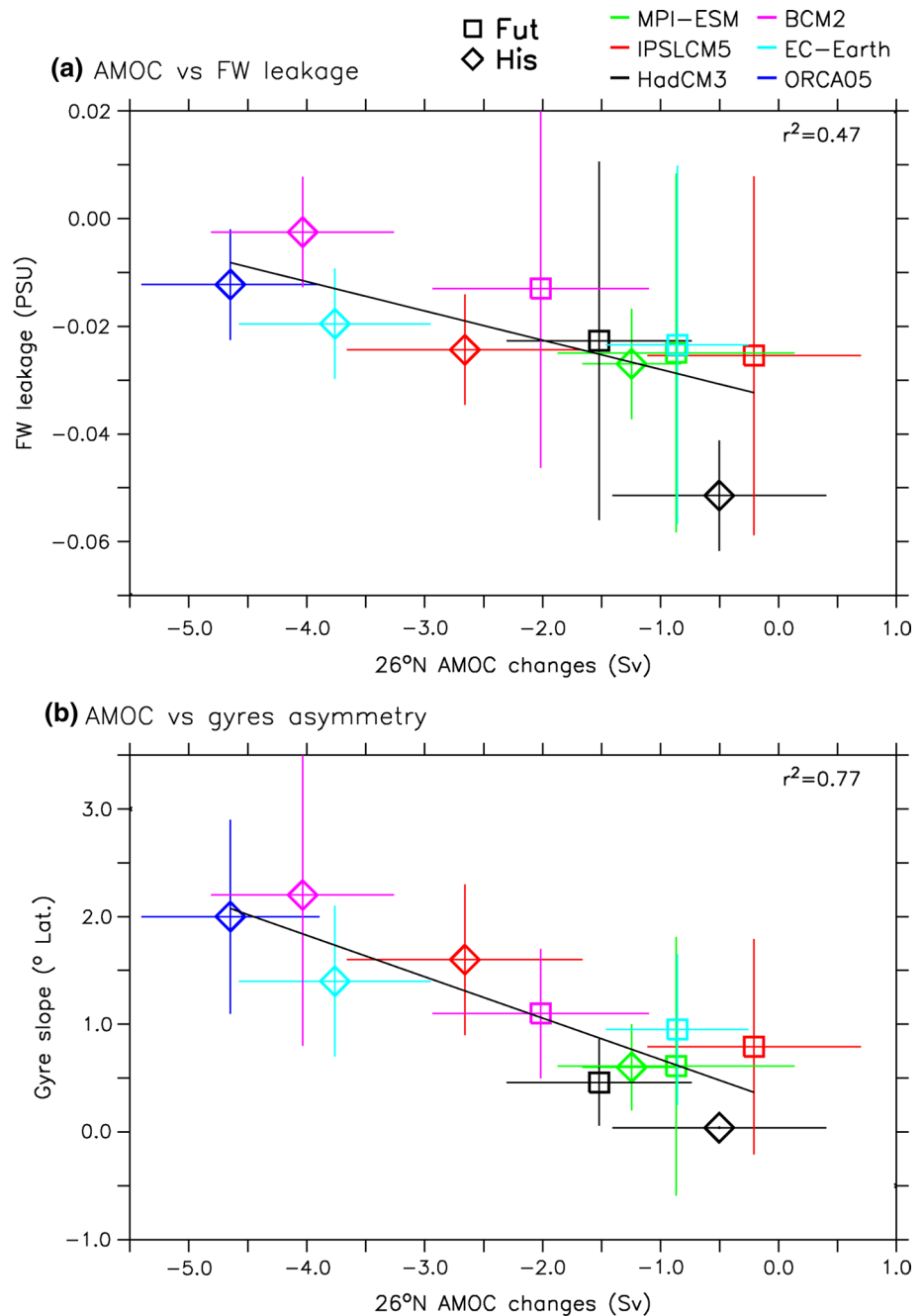
changes serve to reduce the AMOC sensitivity. A partial explanation for the changes in gyre asymmetry can be derived from a northward shift of the storm track paths in the projections. Such an atmospheric response is a known feature already outlined in CMIP3 models (Yin 2005). This northward shift may explain the observed changes in the Ekman pumping (Fig. 13) patterns and shapes, thereby, the gyres structure. The northward shift of the boundary between the subpolar and subtropical gyres is the oceanic response to the atmospheric changes and it is highlighted by the tripole anomaly in the barotropic stream function (Fig. 14). Under the working hypothesis that the gyre symmetry determines leakage strength which influences the amount fresh water that stifles the deep convection, we find a weaker AMOC sensitivity to freshwater input and a reduced multi-model uncertainty in the response under future warming climate conditions (Fig. 7). The impact of gyre asymmetry and freshwater leakage is particularly clear for the BCM2 simulations and also to a smaller extent for HadCM3, IPSLCM5A and EC-Earth. Given that BCM2 experiences a smaller warming compared to the other models, we argue that this increase in leakage in a warmer world could be even larger for a RCP85 scenario, and may further decrease the AMOC sensitivity to freshwater input in this model.

To further test the link between freshwater leakage and advective processes, we use the IPSLCM5 model that shows a reaction in gyre asymmetry changes (Fig. 12) and where the necessary fields are available to properly compute salinity transport. We follow the Swingedouw et al. (2007) approach for the decomposition of the salinity

transport. Both current velocity and salinity in the hosing simulations are decomposed into their mean value in the control simulation and the anomalies with respect to these mean values. This allows evaluating the role of the change of mean state between control and hosing experiments. We focus here on the transport of salinity anomalies by velocity from the control simulation (*cf.* equation 5 from Swingedouw et al. 2007), which is related to the freshwater leakage process described earlier. When computed at 30°N between 50°W and 10°W and down to 1,000 m (corresponding to the location of the Canary Current), this transport increases in the IPSLCM5 model from 1.5×10^6 kg/s for HisHos-HisCon to 1.8×10^6 kg/s for FutHos-FutCon. Such an increase illustrates the intensification of the freshwater leakage in the IPSLCM5 projections and can be related with a strong intensification of the Canary Current of 45 % when computed at 30°N between the coast and 25°W in the first 1,000 m. This confirms what has been found in Fig. 12b. Nevertheless, it still remain unclear why the asymmetry of the gyre is related with the intensity of the leakage through the Canary Current, a topic which deserves a specific study focused on this process.

To explain the increase in the Canary Current, we notice on Fig. 13 that the Ekman-driven subduction is increased along the coast of Africa within the projection, which may increase the current along the coast as well as the upwelling. Such an increase in Ekman suction is pronounced in the IPSLCM5 model and is also consistent in all the other models, indicating that the increase in Canary Current and freshwater leakage may be a robust feature in all the models considered here.

Fig. 12 Figure updated from S2013 with projections and impact simulations (FutCon and FutHos) presented in this paper. **a** AMOC changes versus “freshwater leakage” (FW leakage) averaged over the 4th decade. The AMOC changes are defined as the difference between the melt water impact and control projections for the AMOC maximum at 26°N. FW leakage is defined as the averaged salinity anomaly over the region 20°S–50°N, 50°W–20°E up to 1,000 m depth for the 4 decade. The *black lines* are a least squares linear regression made with the 11 couples of simulations ($r^2 = 0.47$, $p < 0.05$). **b** Same as **a** but for the AMOC changes at 26°N versus the slope of the gyres ($r^2 = 0.77$, $p < 0.01$) computed from a linear regression of the zero line of the barotropic stream function between 45°W–15°W and 40°N–50°N expressed in degrees of latitude for 10° of longitude. The *x* and *y* error bars at the end of each time series represent two standard deviations computed in the control simulations. The *horizontal squares* stand for the new simulations presented in this paper, while the *diamonds* are the simulations points from S2013 (cf. their Fig. 8)



3.6 Bilinear model

In order to disentangle the two processes that seem to explain the weaker sensitivity of the AMOC to freshwater release in a warmer world, we propose a very simple bilinear model. In this model, the AMOC variations are a function of decreasing deep ocean ventilation and gyre asymmetry in the control simulation (slightly affected by hosing, cf. S2013)

$$\Delta AMOC = \lambda \nu + \mu \mathcal{A}$$

where Δ stands for the difference between hosing and control simulation, ν is the ventilated volume in the North

Atlantic defined as the volume of water in the winter mixed layer depth, when deeper than 300 m. \mathcal{A} is the gyre asymmetry in the control experiment. λ and μ are the two parameters determined following a bilinear regression. This simple statistical model implicitly assumes that the two proposed processes are independent, which seems reasonable given the different locations and processes involved. The regression gives the following values for the two parameters: $\lambda = 0.4 \pm 0.032$ nHz and $\mu = 1.8 \pm 0.14$ Sv/Lat, with an $r^2 = 0.83$ (significant at the 99 % threshold using a two-sided t test), which is larger than for the two individual linear models related with each parameter

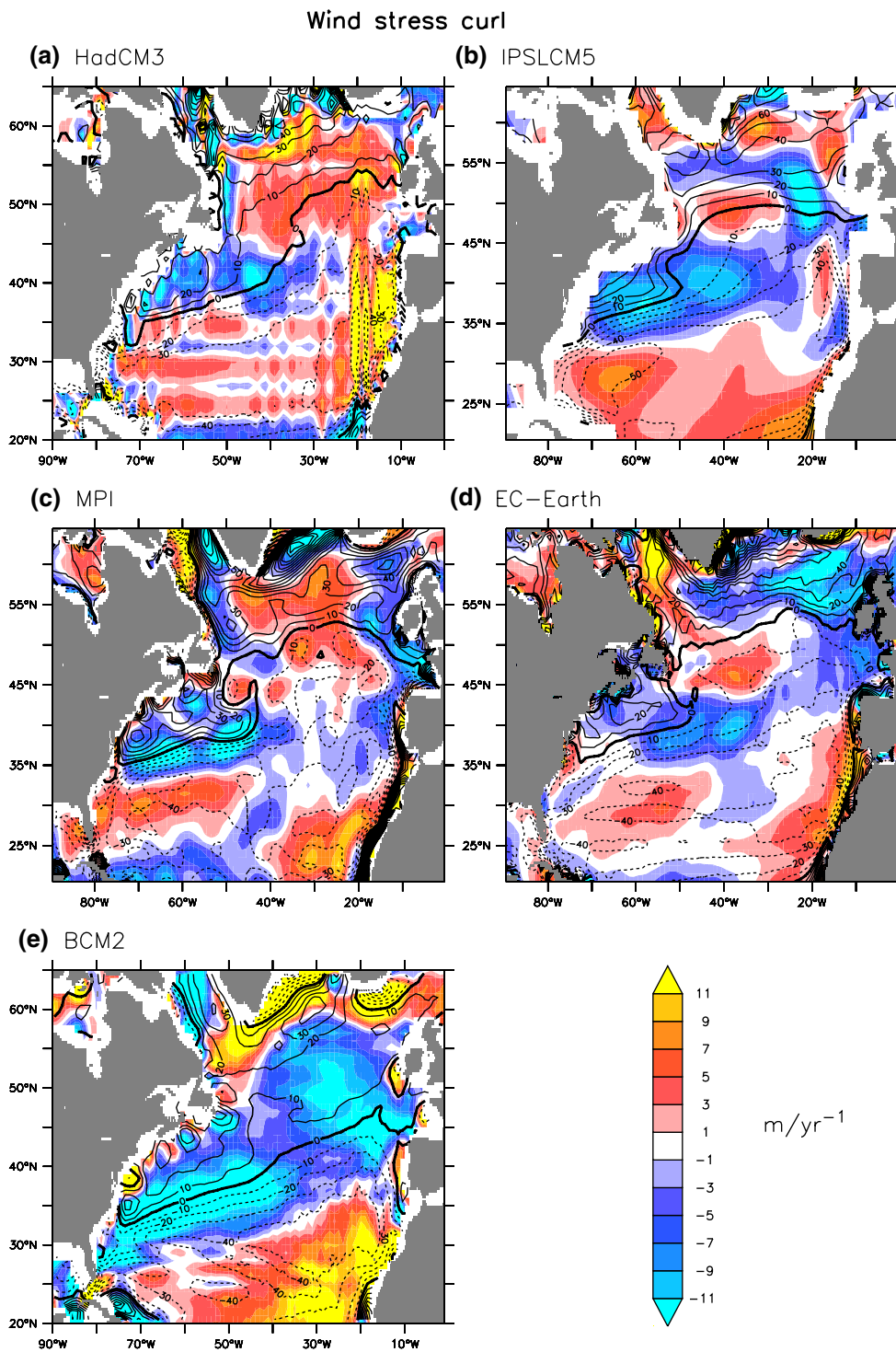


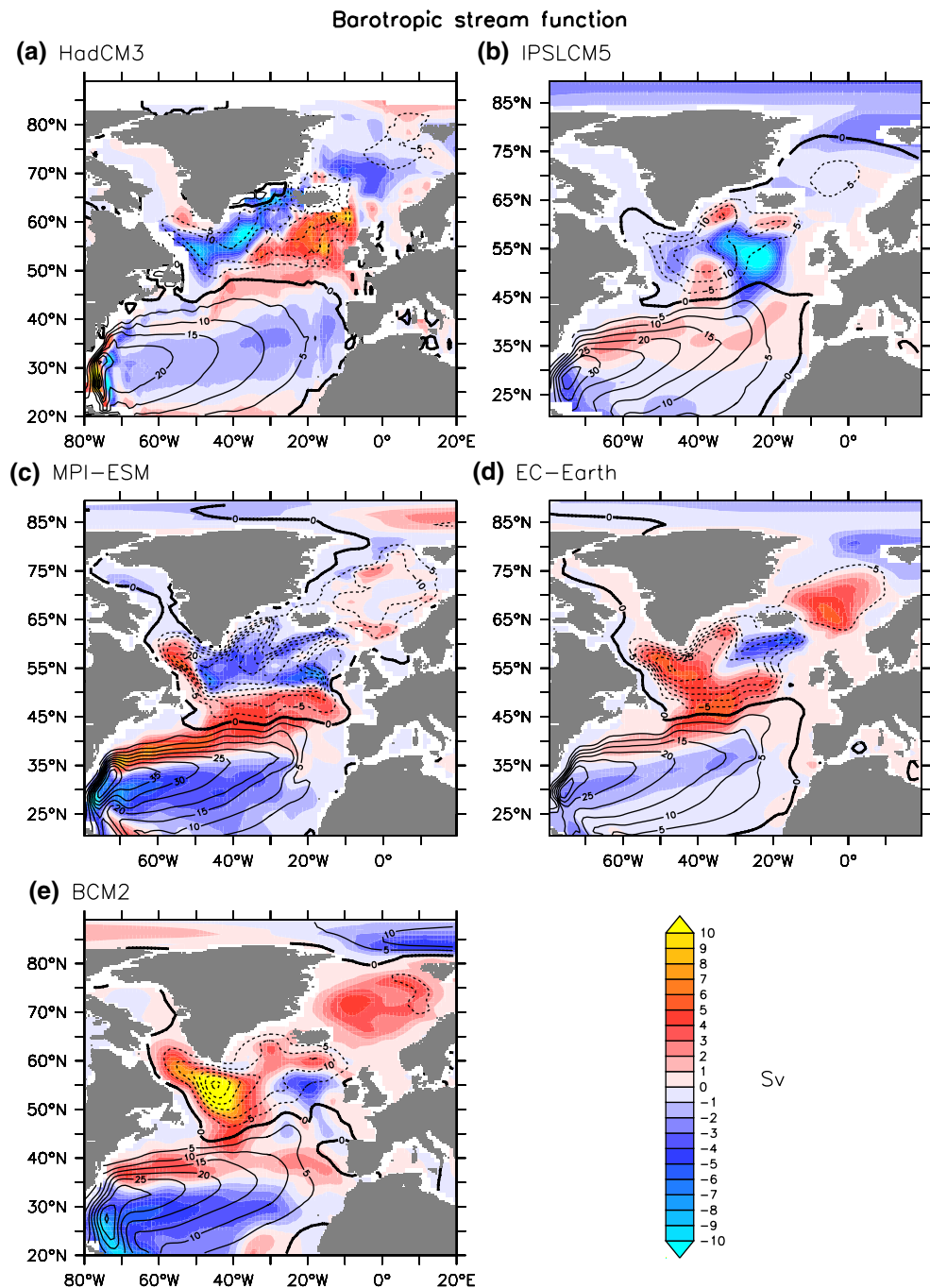
Fig. 13 Difference in wind stress curl (related to Ekman pumping) between control projection (FutCon, 2050–2089) and control historical (HisCon, 1965–2004) experiments averaged over the four decades for the different models (unit: m/year). *Contoured lines* are the

wind stress curl averaged over the period 1964–2004 in the control historical simulations (HisCon, convention for the lines as above). **a** HadCM3, **b** IPSLCM5, **c** MPI-ESM, **d** EC-Earth and **e** BCM2. The colour interval is 2 m/year and the contour line interval is 10 m/year

(Fig. 15). Since the unit of λ is a bit unusual, we notice that it corresponds to the inverse of time constant τ equals to around 80 years.

Although the number of points used to construct this model is small, this model gives an interesting conceptual framework to help discriminating the importance of the

Fig. 14 Difference in barotropic stream function between control projection (FutCon, 2050–2089) and control historical (HisCon, 1965–2004) experiments averaged over the four decades for the different models (unit: Sv). Contoured lines are the barotropic stream function averaged over the period 1964–2004 in the control historical simulations (HisCon, convention for the lines as above). **a** HadCM3, **b** IPSLCM5, **c** MPI-ESM, **d** EC-Earth and **e** BCM2. The colour interval is 1 Sv and the contour line interval is 5 Sv

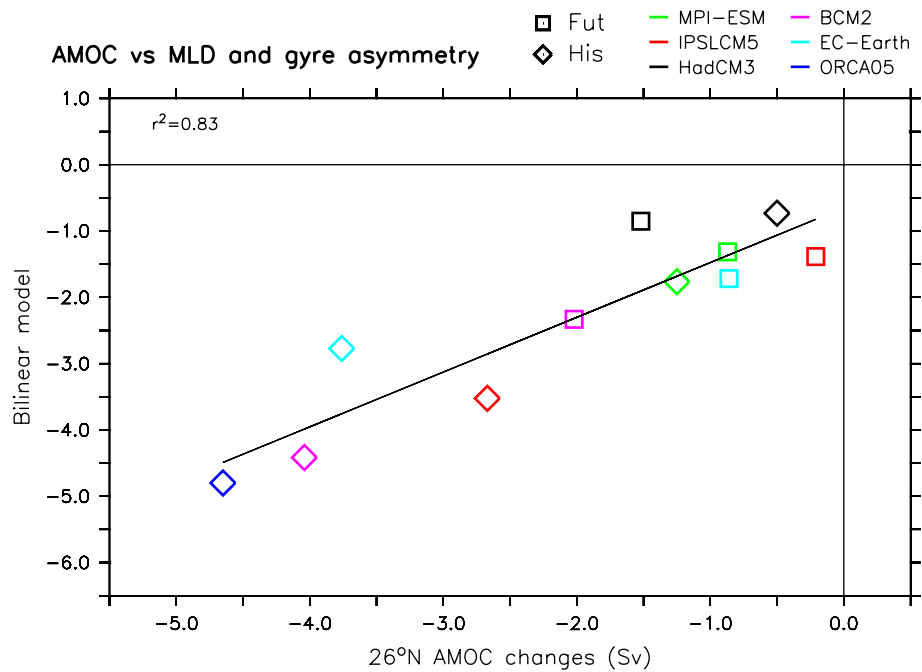


two selected parameters. Indeed, the sensitivity difference between the two sets of historical and future projections simulations is about 1.5 Sv. Following our bilinear model, we compute the part due to gyre asymmetry and the part due to decrease in ventilated volume. For this purpose, we compute the difference of changes in gyre asymmetry between HisCon and FutCon and multiply it by μ to obtain 0.8 Sv. Similarly, we compute the difference in ventilated water in winter between HisHos-HisCon and FutHos-FutCon and multiply it by λ we obtain 0.5 Sv in this second case. The residual of 0.2 Sv, due to not accounted processes by our simple bilinear

model, remains moderate (around 13 % of error). Thus, we obtain that around 62 ± 8 % of the differences between historical and projection sensitivity is due to gyre asymmetry and 38 ± 8 % to decrease in deep ventilation.

Moreover, according to all the former analyses, we notice that the impact of each process is model dependent. Indeed, we can say that the reduction of sensitivity of the AMOC is mainly lead by ventilation saturation process in IPSLCM5 while changes in freshwater leakage may have played a large role in BCM2, HadCM3 and EC-Earth. Changes in sensitivity remain very modest in MPI-ESM.

Fig. 15 Similar to Fig. 9 but here the changes in AMOC at 26°N are plotted versus the results of the bilinear model including changes in ventilation and gyre asymmetry



Nevertheless, the limits of the present bilinear model should be kept in mind, notably associated with the small sample size (only 11 points). For instance, removing ORCA05, an ocean-only model that has been applied only under historical climate conditions, from the bilinear model affects the results slightly. In that case we found $\lambda = 0.34$ nHz and $\mu = 1.77$ Sv/°Lat, with an $r^2 = 0.75$. Nevertheless, this does not change much the main conclusions (the proportions are in that case of 65 and 35 % for the asymmetry and ventilation changes respectively) from this approach, which still relies on strong hypotheses (linearity, link between AMOC and ventilation and gyre asymmetry, independence of the two processes...) and small sampling. Removing other models one by one also leads to very similar coefficients and correlation (standard deviation lower than 20 % for both coefficients).

3.7 Impact on SST

The impact of freshwater input on SST is shown in Fig. 7 (right panels). The dominant fingerprints in the different models, represented by the multi-model mean (Fig. 71), exhibit a similar pattern as under present-day conditions (S2013), with a pronounced cooling of the Atlantic between 0 and 60°N and slight warming in the Nordic Seas and in some parts of the Arctic Ocean. The large-scale cooling of the Atlantic is related to two factors: (1) the decrease in northward heat transport (by more than 0.05 PW at 26°N) associated with the AMOC decline to the imposed GIS melt water as described above, as well as (2) changes in the local stratification due to the decrease in SSS related to the

freshwater release (*cf.* Swingedouw et al. 2009). The latter is the case along the Canary Current, which shallows the mixed layer depth and lowers the vertical heat exchanges.

The continuing advection of subsurface warm Atlantic water masses emerges as warm anomalies in the Nordic Seas, while the fresh water cap isolates the subsurface Atlantic flow from surface conditions. These Atlantic waters are neither ventilated nor cooled in the subpolar gyre, since the freshwater hinders exchange with the surface, which would deliver the heat into the atmosphere. Hence the heat excess re-emerges as a heat anomaly in the Nordic Seas during winter when the mixed layer reaches this Atlantic waters layer. This process already noted in historical conditions (S2013) is still at play in the projections as illustrated in Fig. 6.

4 Conclusions

In this study we have assessed the impact of a strong Greenland ice sheet (GrIS) melting of 0.1 Sv during 40 years on the AMOC under the strong warming scenario RCP8.5 with a multi-model ensemble. None of the models used here simulates a complete shutdown of the AMOC by the applied freshwater discharge, which mimics a high-end melt scenario of the Greenland ice sheet (GrIS). Instead, we uncovered a moderate additional decrease of the AMOC at 26°N of 1.1 ± 0.6 Sv after 40 years of 0.1 Sv hosing between 2050 and 2089 (FutHos) as compared to the experiments with no additional hosing (FutCon). This impact is however reduced compared to identical hosing simulations

under recent historical climate conditions. In addition we have identified a reduced model ensemble spread in the response.

We explain this reduced sensitivity compared to recent historical climate conditions by two main processes. The first one is the decoupling between the surface and the deeper ocean that occurs in the projections across all models. Stratification increases because the surface temperature warms faster than in the layers below. This mitigates the potential effect of any additional freshwater input. Nevertheless, this further weakening of the AMOC related to GrIS melting is associated to a decreasing oceanic heat transport. This impacts the meridional temperature gradient and potentially the localisation of the large-scale climatic structures, in the tropical Atlantic in particular. The second process is related with changes in the mean barotropic circulation in the North Atlantic in the projections compared to historical conditions. This induces a weakening in the freshwater leakage; a process by which the fresh water released around Greenland is removed from the subpolar gyre through the southward flowing Canary Current. Using a very simple conceptual bilinear model calibrated over the whole pool of simulations, we find that around $62 \pm 8 \%$ of the lower AMOC sensitivity is related with changes in gyre asymmetry and $38 \pm 8 \%$ is due to the reduced ventilation in projections as compared to historical simulations.

We argue that more realistic simulations in term of GrIS melting, including iceberg melting location, will help to better estimate its future impact on the AMOC. Here we have shown that this impact in projections may be weaker than anticipated from historical (and potentially preindustrial) climate simulations.

Acknowledgments The research leading to these results has received funding from the European Union's Seventh Framework Programme (FP7/2007-2013) under grant agreement no 212643 (THOR 2008-12), no 282672 (EMBRACE 2011-2015) and no 308299 (NACLIM). CR thanks the DKRZ for providing the facilities to perform the models simulation under the BMWF project bm0579. SMO was partly supported by the Danish Council for Strategic Research. DS benefited of the HPC resources of CCRT made available by GENCI (*Grand Equipement National de Calcul Intensif*). We thank two anonymous reviewers for their very useful comments that improved the manuscript.

References

- Bamber J, van den Broeke M, Etema J, Lenaerts J, Rignot E (2012) Recent large increases in freshwater fluxes from Greenland into the North Atlantic. *Geophys Res Lett* 39:L19501. doi:[10.1029/2012GL052552](https://doi.org/10.1029/2012GL052552)
- Belkin IM, Levitus S, Antonov J, Malmberg S-A (1998) "Great Salinity Anomalies" in the North Atlantic. *Prog Oceanogr* 41:1–68
- Driesschaert E, Fichefet T, Goosse H, Huybrechts P, Janssens I, Mouchet A, Munhoven G, Brovkin V, Weber SL (2007) Modelling the influence of Greenland ice sheet melting on the Atlantic meridional overturning circulation during the next millennia. *Geophys Res Lett* 34:L1070
- Durack PJ, Wijffels SE, Matear RJ (2012) Ocean salinities reveal strong global water cycle intensification during 1950 to 2000. *Science* 336(6080):455–458. doi:[10.1126/science.1212222](https://doi.org/10.1126/science.1212222)
- Fichefet T, Poncin C, Goosse H, Huybrechts P, Janssens I, Treut HL (2003) Implications of changes in freshwater flux from the Greenland ice sheet for the climate of the 21st century. *Geophys Res Lett* 30:1911. doi:[10.1029/2003GL017826](https://doi.org/10.1029/2003GL017826)
- Ganopolski A, Rahmstorf S (2001) Rapid changes of glacial climate simulated in a coupled climate model. *Nature* 409(6817)
- Gregory JM et al (2005) A model intercomparison of changes in the Atlantic thermohaline circulation in response to increasing atmospheric CO₂ concentration. *Geophys Res Lett* 32:L12703
- Hu A, Meehl GA, Han W, Yin J (2011) Effect of the potential melting of the Greenland ice sheet on the meridional overturning circulation and global climate in the future. *Deep Sea Res Part II* 58(17–18):1914–1926. doi:[10.1016/j.dsr2.2010.10.069](https://doi.org/10.1016/j.dsr2.2010.10.069)
- Jungclauss JH, Haak H, Esch M, Roeckner E, Marotzke J (2006) Will Greenland melting halt the thermohaline circulation? *Geophys Res Lett* 33 (Article Number: L17708)
- Kanzow T, Cunningham SA, Johns WE, Hirschi JJ-M, Marotzke J, Baringer MO, Meinen CS, Chidichimo MP, Atkinson C, Beal LM, Bryden HL, Collins J (2010) Seasonal variability of the Atlantic meridional overturning circulation at 26.5°N. *J Clim* 23:5678–5698. doi:[10.1175/2010JCLI3389.1](https://doi.org/10.1175/2010JCLI3389.1)
- Levitus S et al (1998) Introduction, vol 1. World Ocean Database 1998. NOAA Atlas NESDIS 18, NOAA/NESDIS. U.S. Dept. of Commerce, Washington, DC
- Mikolajewicz U, Voss R (2000) The role of the individual air-sea flux components in CO₂-induced changes of the ocean's circulation and climate. *Clim Dyn* 16:627–642
- Mikolajewicz U, Vizzafo M, Jungclauss J, Schurgers G (2007) Effect of ice sheet interactions in anthropogenic climate change simulations. *Geophys Res Lett* 34:L18706. doi:[10.1029/2007GL031173](https://doi.org/10.1029/2007GL031173)
- Morita T et al (2011) 2.5.1.1 IPCC Emissions Scenarios and the SRES Process, in IPCC TAR WG3 2001
- Moss RH, Edmonds JA, Hibbard KA, Manning MR, Rose SK et al (2010) The next generation of scenarios for climate change research and assessment. *Nature* 463:747–756
- Ridley JK, Huybrechts P, Gregory JM, Lowe JA (2005) Elimination of the Greenland ice sheet in a high CO₂ climate. *J Clim* 18:3409–3427
- Rignot E, Velicogna I, van den Broeke MR, Monaghan A, Lenaerts J (2011) Acceleration of the contribution of the Greenland and Antarctic ice sheets to sea level rise. *Geophys Res Lett* 38:L05503
- Schneider B, Latif M, Schmittner A (2007) Evaluation of different methods to assess model projections of the future evolution of the Atlantic meridional overturning circulation. *J Clim* 20:2121–2132
- Schrama EJO, Wouters B (2011) Revisiting Greenland ice sheet mass loss observed by GRACE. *J Geophys Res* 116:B02407. doi:[10.1029/2009JB006847.5267](https://doi.org/10.1029/2009JB006847.5267)
- Stouffer RJ, Yin J, Gregory JM, Dixon KW, Spelman MJ, Hurlin W, Weaver AJ, Eby M, Flato GM, Hasumi H, Hu A, Jungclauss JH, Kamenkovich IV, Levermann A, Montoya M, Murakami S, Nawrath S, Oka A, Peltier WR, Robitaille DY, Sokolov A, Vettoretti G, Weber SL (2006) Investigating the causes of the response of the thermohaline circulation to past and future climate changes. *J Clim* 19:1365–1387
- Swingedouw D, Braconnot P, Marti O (2006) Sensitivity of the Atlantic meridional overturning circulation to the melting from northern glaciers in climate change experiments. *Geophys Res Lett* 33 (Art. No. L07711)
- Swingedouw D, Braconnot P, Delecluse P, Guilyardi E, Marti O (2007) Quantifying the AMOC feedbacks during a 2×CO₂ stabilization

- experiment with land-ice melting. *Clim Dyn* 29(5):521–534. doi:[10.1007/s00382-007-0250-0](https://doi.org/10.1007/s00382-007-0250-0)
- Swingedouw D, Mignot J, Braconnot P, Mosquet E, Kageyama M, Alkama R (2009) Impact of freshwater release in the North Atlantic under different climate conditions in an OAGCM. *J Clim* 22:6377–6403
- Swingedouw D, Rodehacke C, Behrens E, Menary M, Olsen S, Gao Y, Mikolajewicz U, Mignot J, Biastoch A (2013) Decadal fingerprints of fresh water discharge around Greenland in a multi-models ensemble. *Clim Dyn*. doi:[10.1007/s00382-012-1479-9](https://doi.org/10.1007/s00382-012-1479-9)
- Van Meerbeeck CJ, Roche DM, Renssen H (2011) Assessing the sensitivity of the North Atlantic Ocean circulation to freshwater perturbation in various glacial climate states. *Clim Dyn* 37(9–10):1909–1927. doi:[10.1007/s00382-011-1043-z](https://doi.org/10.1007/s00382-011-1043-z)
- Vizcaíno M, Mikolajewicz U, Jungclaus J, Schurgers G (2010) Climate modification by future ice sheet changes and consequences for ice sheet mass balance. *Clim Dyn* 34(2–3):301–324. doi:[10.1007/s00382-009-0591-y](https://doi.org/10.1007/s00382-009-0591-y)
- Weaver AJ, Sedláček J, Eby M, Alexander K, Crespin E, Fichefet T, Philippon-Berthier G, Joos F, Kawamiya M, Matsumoto K, Steinacher M, Tachiiri K, Tokos K, Yoshimori M, Zickfeld K (2012) Stability of the Atlantic meridional overturning circulation: a model intercomparison. *Geophys Res Lett* 39:L20709. doi:[10.1029/2012GL053763](https://doi.org/10.1029/2012GL053763)
- Winguth A, Mikolajewicz U, Gröger M, Maier-Reimer E, Schurgers G, Vizcaíno M (2005) Centennial-scale interactions between the carbon cycle and anthropogenic climate change using a dynamic earth system model. *Geophys Res Lett* 32(23). doi:[10.1029/2005GL023681](https://doi.org/10.1029/2005GL023681)
- Wood RA, Keen AB, Mitchell JFB, Gregory JM (1999) Changing spatial structure of the thermohaline circulation in response to atmospheric CO₂ forcing in a climate model. *Nature* 399:572–575
- Yin JH (2005) A consistent poleward shift of the storm tracks in simulations of 21st century climate. *Geophys Res Lett* 32:L18701